

A study of the electronic structures of Pd_2^- and Pd_2 by photoelectron spectroscopy

Joe Ho, Kent M. Ervin,^{a)} Mark L. Polak, Mary K. Gilles, and W. C. Lineberger
Department of Chemistry and Biochemistry, University of Colorado, and Joint Institute for Laboratory Astrophysics, University of Colorado and National Institute of Standards and Technology, Boulder, Colorado 80309-0440

(Received 7 June 1991; accepted 25 June 1991)

The ultraviolet negative ion photoelectron spectrum of Pd_2^- is presented for electron binding energies up to 3.35 eV. The anion is prepared by sputtering in a flowing afterglow ion source. Multiple low-lying electronic states of Pd_2 , all unidentified previously, are observed with resolved vibrational structure. The spectrum shows two strong electronic bands, each with similar vibrational progressions. Franck-Condon analyses are carried out on the two transitions and molecular constants are extracted for the anion and the two neutral electronic states. With the help of simple molecular orbital arguments and *ab initio* calculations, these two electronic bands are assigned as the triplet ground state ($^3\Sigma_u^+$) and a singlet excited state ($^1\Sigma_u^+$). The adiabatic electron affinity is $\text{E.A.}(\text{Pd}_2) = 1.685 \pm 0.008$ eV and the singlet excitation energy $T_0(^1\Sigma_u^+)$ is 0.497 ± 0.008 eV (4008 ± 65 cm^{-1}). The bonding in the palladium dimers is discussed and we find that the anion bond strength is 1.123 ± 0.013 eV stronger than that of the neutral. Related studies of Pd^- yield an improved electron affinity of $\text{E.A.}(\text{Pd}) = 0.562 \pm 0.005$ eV.

I. INTRODUCTION

Small transition metal clusters have been studied intensively in recent years.¹⁻³ The motivations for these studies include understanding the catalytic nature of metal surfaces and mapping the transition between molecular properties and metallic behavior. The goal of understanding the nature of the metal-metal bond has also stimulated studies of metal clusters.⁴ The availability of *d* electrons for chemical bonding makes transition metal clusters both interesting and complex. Spectroscopic investigations of small transition metal clusters provide rich information on electronic and vibrational structure, and metal-metal bonding properties.

The coinage metal dimers (Cu_2 , Ag_2 , and Au_2) are presently well characterized.¹⁻⁷ Because of the simple closed *d*-shell configurations ($d^{10}s^1$) in the atomic ground states, the electronic structures and the bonding in the dimers are determined mainly by the valence *s* electron interactions. The nickel group dimers are still relatively simple compared to other transition metals since there is only one *d* hole (Ni and Pt), or a fully filled *d* shell (Pd) in the ground electronic configuration of the constituent atoms. These dimers should be similar to the neighboring coinage metal dimers in that the interactions of the *s* electrons dominate the bonding and the electronic structure of the dimers. However, since the *s* and *d* orbitals have similar energies, the *d* electrons may participate in the bonding as well.⁷ By comparing bonding properties between the nickel group and the well-studied coinage metal dimers, we can obtain insight into the participation of *d* electrons in metal bonding. In addition, the nickel group metal dimers can serve as a starting point for systematic studies of open *d*-shell transition metal dimers.

Theoretical investigations on Ni_2 ,⁸ Pd_2 ,⁹⁻¹² and Pt_2 ,^{9,13} and gas phase spectroscopic experiments on Ni_2 ,¹⁴ Pt_2 ,¹⁵ and on heteronuclear dimers (NiPd , NiPt , and PdPt)^{16,17} have been reported.

Pd occupies a special position among the transition metals because of its unique ground state atomic configuration $^1S_0(4d^{10}5s^0)$. In a first-order approximation, the combination of the two closed-shell Pd atoms (1S_0) only forms a weak van der Waals bond, so the two ground state palladium atoms cannot be strongly bound in the dimer. To increase the bonding, at least one *4d* electron must be excited to a *5s* orbital on one or both atoms. The interaction of an excited $^3D(4d^95s^1)$ atom with a ground state atom forms an *σσ* bond with a formal bond order of one-half, but the promotion energy required¹⁸ is 6564 cm^{-1} . Likewise, two 3D atoms can generate a bound state, but twice the promotion energy is required for a bond order of one. Because of this complicated situation, the electronic structures of the Pd_2 ground and low-lying excited electronic states are not well characterized. Spectroscopic studies of the Pd_2 low-lying electronic states can help reveal the nature of the metal bond.

Pd_2 has been investigated theoretically at a variety of levels. Basch *et al.*⁹ used a relativistic effective core potential (ECP) and a limited multiconfiguration self-consistent field (MCSCF) method; Shim and Gingerich¹⁰ employed a non-relativistic all-electron Hartree-Fock (HF)/valence configuration interaction (CI) calculation; and Salahub¹¹ applied model-potential methods with relativistic corrections. All of the studies have demonstrated the complexity of the Pd_2 electronic structure, but they vary with respect to the ground state assignments and the energies of the many low-lying electronic states.¹ Balasubramanian¹² recently carried out a complete active space MCSCF (CASSCF) calculation followed by multireference single and double CI (MRSDCI)

^{a)} Present Address: Department of Chemistry, University of Nevada, Reno, NV 89557.

and relativistic CI to calculate properties of the low-lying electronic states of Pd₂. This calculation employed the largest basis set used to date. It also employed a spin-orbit correction and included 41 electronic states below 9000 cm⁻¹. A ³Σ_u⁺ (1_u) ground state and an antiparallel spin coupling state ¹Σ_u⁺ at 4443 cm⁻¹ are predicted. Lee *et al.*¹⁹ calculated the spectroscopic parameters of Pd₂ using local-spin-density (LSD) theory and a full relativistic norm-conserving pseudopotential and predicted a ³Σ_u⁺ ground state with a vibrational frequency of 222 cm⁻¹.

In contrast, relatively little experimental data have been reported. High temperature measurements using Knudson effusion mass spectrometry²⁰ give a second-law value of $D_0(\text{Pd}_2) = 1.13 \pm 0.22$ eV. Coupled with *ab initio* calculations, a reinvestigation¹⁰ of this experiment provided a third-law value of $D_0(\text{Pd}_2) = 1.03 \pm 0.16$ eV. Spectroscopic experiments on palladium dimer are almost nonexistent. Quite recently, the Morse group has attempted two-photon ionization spectroscopy of gas phase Pd₂, but no transitions were observed in their scanning range.¹⁷ They proposed that efficient predissociation prevents observation by their experimental technique. To our knowledge, no other gas-phase spectroscopic studies on Pd₂ have been reported.

In this paper, we present the ultraviolet (351.1 nm or 3.531 eV) photoelectron spectrum of the palladium dimer anion Pd₂⁻. Previous reports from this laboratory involved visible (488.0 nm or 2.540 eV) photoelectron spectra of the copper metal clusters²¹ (Cu_n⁻, $n = 1-10$), the nickel group trimers²² (Ni₃⁻, Pd₃⁻, and Pt₃⁻), and the near ultraviolet (351.1 nm) photoelectron spectra of the coinage group metal clusters⁶ (Cu_n⁻, Ag_n⁻, and Au_n⁻). Several factors make negative ion photoelectron spectroscopy a powerful technique for the study of small metal clusters. First, since the cluster anions are separated with a mass spectrometer, the identity of the cluster giving rise to the photoelectron spectrum^{23,24} is unambiguous. Second, the neutral ground state and low-lying excited electronic states are accessible through transitions from the anion ground state. Third, the spin selection rule for photodetachment is $\Delta S = \pm 1/2$ and the energy splitting between states of different multiplicity, e.g., a singlet-triplet splitting can be measured directly. Additionally, the 9–10 meV (70–80 cm⁻¹) instrumental resolution is adequate to resolve the vibrational properties of dimeric transition metal clusters, which typically possess frequencies in the range of 100–500 cm⁻¹. Finally, the measurement of photoelectron angular distributions offers a sensitive probe of the molecular orbitals.²⁵ This measurement provides information which is helpful in identifying the anion and neutral ground states and which also aids in understanding the properties of the metal-metal bond.

In Sec. II, we review the experimental methods used in this study. Photoelectron spectra are presented in Sec. III, along with the results of photoelectron angular distribution measurements. A Franck-Condon analysis and spectral simulation yields the electron affinity, vibrational constants, and bond length changes. The photoelectron spectrum of the atomic anion Pd⁻ has also been recorded, yielding an improved atomic electron affinity. Section IV contains a discussion of the electronic configurations and the bonding in

the anion and neutral ground states. The discussion also extends to the neutral low-lying electronic excited states. The anion and neutral ground states and a low-lying excited state of the neutral are assigned according to simple molecular orbital (MO) arguments. Our experimental results are compared with the *ab initio* calculations and show good agreement. A comparison of the palladium dimer with the nickel, platinum, and coinage metal dimers is included in the discussion.

II. EXPERIMENTAL METHODS

The negative ion photoelectron spectrometer^{23,24} and metal cluster anion source^{6,21} have been described in detail previously. Briefly, the palladium atom and dimer anions are produced in a flowing afterglow ion source by cathodic sputtering with a dc discharge. A mixture of 10%–20% argon (ultrahigh purity) in helium (99.999%) flows over the metal cathode at a flow tube pressure of ~0.4 Torr. The cathode is fabricated from high purity (> 99.9%) palladium foil and the corresponding cluster anions are produced from sputtering of the metal cathode by Ar⁺ and other cations. The cathode is negatively biased, typically at 3–4 kV with respect to the grounded flow tube, producing a discharge with a current of 10–30 mA. The gas composition, flow rate, and dc voltage are adjusted to optimize the cluster anion yields.

The ions are extracted from the flow tube into a low pressure region, then focused into a beam and mass selected by a Wien filter. The mass resolution of the Wien filter ($M/\Delta M = 40-50$) allows us to separate the bare metal clusters from their oxides. The mass selected ion beam is further focused and then sent into the interaction region. The ion current is monitored by a Faraday cup just behind the interaction region. The ion beam is crossed by a cw laser beam with a wavelength of 351.1 nm (3.531 eV), which induces photodetachment in a fraction of the anions. The interaction region is in the center of an optical build-up cavity which provides internal circulating powers of 30–40 W from incident argon ion laser powers of 150–200 mW.²⁵ Photoelectrons ejected into a small solid angle are collected perpendicularly to the plane of the ion and laser beams, and their kinetic energies are measured in a hemispherical electrostatic energy analyzer.²³ The electron kinetic energy scale is calibrated with respect to the precisely known electron affinity of atomic oxygen.²⁶ Spectra are further corrected for an energy scale compression factor²³ calibrated on the known energy level spacings of the palladium and tungsten atoms.¹⁸ The electron binding energy (eBE) is determined from the photon energy ($h\nu$) minus the measured electron kinetic energy (eKE). The instrumental resolution function of the photoelectron spectrometer is determined by observing the shapes of atomic transitions and can be approximated by a Gaussian with a 9–10 meV full width at half-maximum (FWHM). The experimental uncertainty of the absolute electron kinetic energy of well-resolved peaks is ± 0.006 eV.

Since the direction of the ejected electron detection is fixed, the angle between the electron detection and the electric field of laser light can be changed conveniently by rotat-

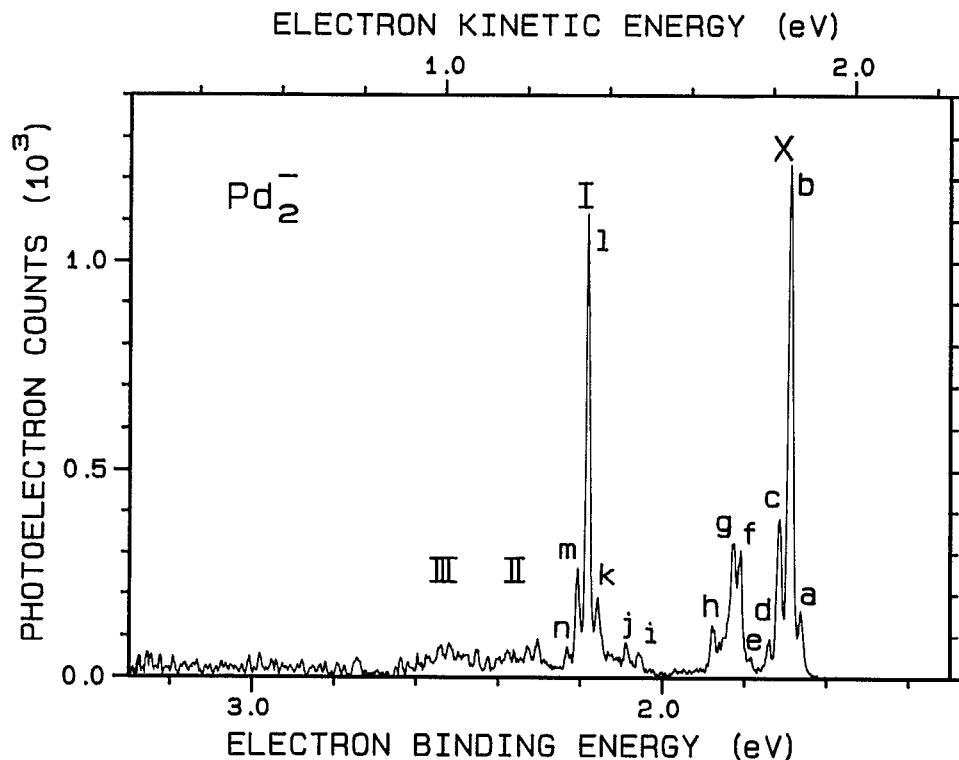


FIG. 1. Photoelectron spectrum of Pd₂⁻ at 351.1 nm (3.53 eV) with 9–10 meV instrumental resolution. The photoelectron spectrum was taken at the “magic” angle $\theta = 54.7^\circ$ and the photoelectron counts are plotted as a function of the electron binding energy ($eBE = h\nu - eKE$).

ing a $\lambda/2$ waveplate which is external to the laser build-up cavity.²⁵ The photoelectron angular distribution can be determined by measuring the photodetachment cross section as a function of the direction of the laser polarization. The angular distribution of the photoelectron intensity with linearly polarized light is given by²⁷

$$d\sigma/d\Omega = (\sigma/4\pi) [1 + \beta(3 \cos^2\theta - 1)/2], \quad (1)$$

where θ is the angle between the laser electric field and the direction of electron collection, σ is the total photodetachment cross section, and β is the asymmetry parameter which varies from -1 to 2 . The photoelectron spectrum in Fig. 1 is taken at the magic angle of $\theta = 54.7^\circ$, for which the anisotropic term is zero, giving intensities proportional to the total photodetachment cross section, regardless of the value of β .

III. RESULTS AND ANALYSIS

A. Photoelectron spectra

The photoelectron spectrum of the atomic anion Pd⁻ was recorded at a resolution improved by a factor of 6 over that obtained in the previous study.²⁸ The electron kinetic energy scale of the Pd⁻ spectrum is calibrated with respect to the precisely known²⁶ electron affinity of atomic oxygen. The new atomic electron affinity is measured to be 0.562 ± 0.005 eV, which is consistent with the prior result (0.557 ± 0.008 eV).²⁸ In addition, the first excited state of Pd⁻, i.e. $^2D_{5/2}(4d^95s^2)$ is found to be 0.138 ± 0.008 eV (1113 ± 65 cm⁻¹) above the anion ground state $^2S_{1/2}(4d^{10}5s)$, slightly higher than the value in the original study.²⁸

The photoelectron spectrum of Pd₂⁻ is shown in Fig. 1. The intensity of the spectrum is shown as a function of the electron binding energy in the range 1.3–3.3 eV. No transitions were observed below 1.3 eV electron binding energy. The spectrum exhibits rich structure comprising abundant vibrational and electronic transitions. The widths of the vibrational peaks are in the range of 10–25 meV, significantly broader than the instrumental linewidth. Rotational contour modeling²⁹ predicts that rotational broadening contributes less than 1 meV to the observed widths. The presence of vibrationally and possibly electronically excited anions, overlapping low-lying neutral electronic excited states, and spin-orbit splittings may all contribute to the observed linewidths.

Fourteen prominent peaks are labeled by letters in Fig. 1 and the peak positions are listed in Table I. The two strongest electronic transitions stand out in the spectrum: the vibrational peaks *a*, *b*, *c*, and *d* form an electronic band and peaks *l*, *m*, and *n* form another band. The two bands have nearly identical Franck–Condon vibrational profiles and transition intensities. Since no transition appears below the peak *a*, the band with low electron binding energy is labeled *X* and is assigned to the neutral ground state. The other intense band is labeled *I* for reference. There are several peaks lying between the *X* and *I* bands. These peaks *e*–*j* are all relatively weak and partially overlap one another. Peaks *f* and *g* have approximately the same intensities and the spacing between them is 125 cm⁻¹. The spacing between peaks *g* and *h* is 400 cm⁻¹, much larger than the expected value for a single vibrational spacing of Pd₂. From the peak spacings and the intensity distribution, it is certain that more than one

TABLE I. Electron binding energies and asymmetry parameters of Pd₂ - Pd₂⁻ transitions.

Band ^a	Peak ^b	Transition		eBE ^c (eV)	β
		ν'	ν''		
X	a	0	1	1.661 ± 0.010	
	b	0	0	1.687 ± 0.008	1.7 ± 0.2
	c	1	0	1.714 ± 0.010	
	d	2	0	1.739 ± 0.010	
	e			1.784 ± 0.015	
	f			1.810 ± 0.010	1.5 ± 0.3
	g			1.825 ± 0.010	1.5 ± 0.3
	h			1.875 ± 0.010	~ 1.3
	i			2.054 ± 0.015	~ -0.1
	j			2.086 ± 0.015	~ -0.4
I	k ^d			2.156 ± 0.015	~ -0.3
	l	0	0	2.182 ± 0.008	1.5 ± 0.3
	m	1	0	2.205 ± 0.010	
	n	2	0	2.229 ± 0.015	
II			2.25 - 2.41	~ -0.2	
III			2.41 - 2.61	~ -0.1	

^a Bands are labeled in Fig. 1.

^b Prominent vibrational peaks are labeled in Fig. 1.

^c The electron binding energy is determined by Franck-Condon simulations for peaks *b* and *l*, and at the intensity maximum for all other peaks.

^d Peak *k* overlaps with the hot band transition (ν' ← ν'') of band *I* (see the text).

electronic state is responsible for these peaks. We assign peaks *f*, *g*, and *h* to three different electronic states and peak *e* to a hot band transition. For peaks *i* and *j*, the intensities are even weaker and the spacing between these two peaks is 250 cm⁻¹. At present, it is unclear whether peaks *i* and *j* arise from the same or different electronic states.

On the high electron binding energy side of the *I* band, there are two groups of weak transitions *II* (2.25–2.41 eV) and *III* (2.41–2.61 eV). Each group appears to contain vibrational structure, but the spacings between the vibrational peaks and the intensity distributions of these peaks are irregular. More than a single electronic transition could be responsible for each feature. In the region of 2.6–3.3 eV, the spectrum shows very weak and structureless features. These features may arise from numerous weak electronic transitions and possibly extend into the low energy region, but are hidden by the other labeled peaks. We have not attempted to assign these features.

B. Angular distributions

The measurements of the angular distributions were performed by taking the photoelectron spectrum over the entire energy range at θ = 0° and θ = 90°. The measured intensities are normalized by the integration time, ion current, and laser power. The asymmetry parameter β for each transition can be estimated by

$$\beta = \frac{(I_0 - I_{90})}{[(1/2)I_0 + I_{90}]}, \quad (2)$$

where *I*₀ and *I*₉₀ are the normalized intensities at θ = 0° and θ = 90°. The measured β values are listed in Table I. The

intensities are measured for the individual vibrational peaks. For bands *X* and *I*, the measurements indicate that all of the vibrational transitions within a single electronic state have approximately the same β value as the origin. The β values of bands *X* and *I* are 1.7 ± 0.2 and 1.5 ± 0.3, and β ≈ 1.5 for peaks *f*, *g* and *h*. The β values for peaks *i* and *j* and features *II* and *III* are all negative. Although peak *k* can be assigned to the hot band transition (ν' = 0 ← ν'' = 1) of band *I* based upon its position, a negative β is measured, making this assignment unlikely. The β difference between peak *k* and the peaks (*l*, *m*, and *n*) in band *I* indicates that there is another independent peak which overlaps the hot band transition of band *I*. The angular distribution measurement aids in distinguishing overlapping bands or peaks if their β values are very different.^{25,30}

Early negative ion photoelectron spectroscopy experiments³¹ showed that β = 2 for *s* orbital detachment from H⁻. Similar measurements were performed on several alkali metal³² and transition metal³³ atoms and confirmed that β = 2 for atomic transitions arising from pure *s* electron detachment. If the transition arises from *d*-electron detachment and the transition is not very close to threshold, β is usually a negative value. Recently, angular distribution measurements were also performed on the coinage metal dimers.³³ For Ag₂⁻, which is in the same row of the Periodic Table as Pd₂⁻, two transitions corresponding to X¹Σ_g⁺ (σ_g²) ← X²Σ_u⁺ (σ_g²σ_u¹) and a³Σ_u⁺ (5sσ_g¹σ_u¹) ← X²Σ_u⁺ (σ_g²σ_u¹) were observed.⁶ Removal of one 5sσ_u electron corresponds to the ground to ground state transition and the measured β for this band is 0.8 ± 0.3; removal of a 5sσ_g electron corresponds to an excited state transition, and β for this band is 1.5 ± 0.3. The experiments show that the Ag₂ 5sσ_g orbital is almost spherically symmetric, while 5sσ_u electron detachment is not as strongly peaked along the electric vector. One possible explanation is based on the orbital symmetry. In contrast to the σ_g orbital, the σ_u orbital is antisymmetric (*p* like) with respect to the reflection through the central plane perpendicular to the molecular axis.

By simple analogy, the angular distributions in the present measurements imply that there are two kinds of photoelectron processes in the Pd₂ spectrum, one with β > 1 corresponding to *s*-like or *sσ* electron detachment, such as *X*, *I*, *e*, *f*, *g*, and *h*; others with negative β corresponding to *d*-like electron detachment, i.e., *i*, *j*, *k*, *II*, and *III*. We will discuss this assignment in more detail in Sec. IV.

C. Franck-Condon analysis

Franck-Condon analyses were applied to the *X* and *I* bands in the Pd₂⁻ spectrum. The method of our Franck-Condon analysis has been described previously.⁶ First, we will summarize the simulation of band *X*. Since no molecular parameters for the neutral or anion have been determined experimentally, we fit both the anion and neutral molecular constants simultaneously. Optimizing the simulated spectrum to the experimental data with a nonlinear least-squares fit determines the position of the transition origin, the bond length change, vibrational frequencies for both the anion

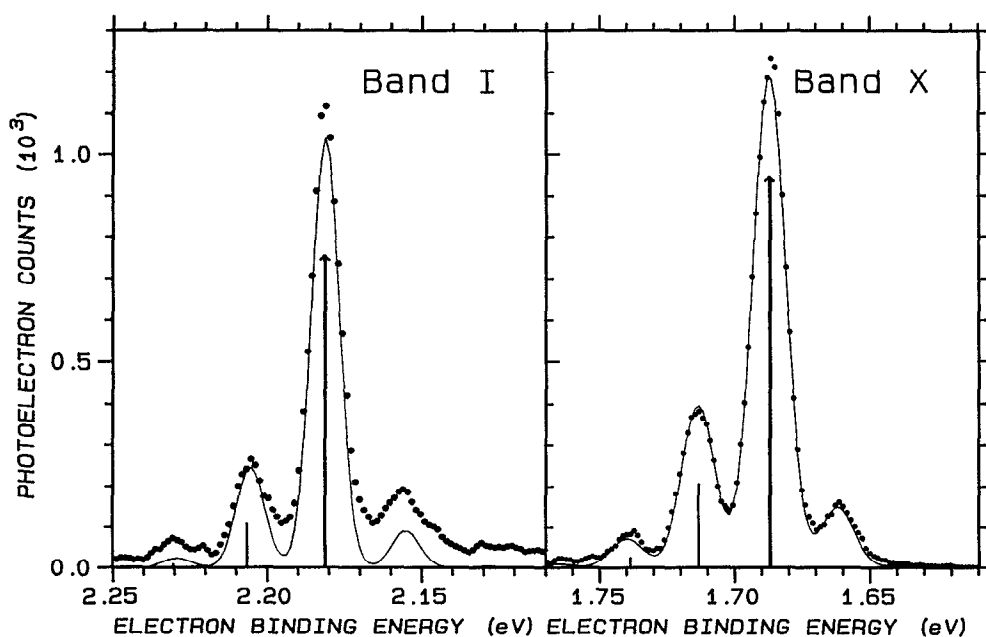


FIG. 2. Expanded portions of the *X* and *I* bands of the Pd₂⁻ spectrum. The points represent the experimental data and the solid curves are the optimized Franck–Condon simulations. The transitions from the anion vibrational ground state are given by the vertical sticks. Arrows mark the transition origins ($v' = 0 \leftarrow v'' = 0$). The fit for band *I* is not as good as that for band *X*, due to the overlap of the electronic transitions.

and neutral molecules, and the anion vibrational temperature. The expanded spectrum of the *X* band and the optimized fit are shown in Fig. 2. This determination of the transition origin gives a first approximation to the adiabatic electron affinity of $E.A.(Pd_2) = 1.687 \pm 0.008$ eV. This value will be slightly modified for some spin–orbit effects in Sec. IV. The anion vibrational temperature is determined to be 300 ± 25 K. The rotational temperature cannot be measured directly, but is usually equal to or lower than the vibrational temperature, because rotational relaxation by collisions with the buffer gas in the ion source is more efficient than vibrational relaxation.^{24,34}

The *I* band simulation is slightly different from that of the *X* band. The anion molecular constants (ω_e'' and T_{vib}) obtained above were employed and constrained during the simulation. The fit of band *I* shown in Fig. 2 is not as good as that of band *X*, because band *I* is overlapped with other states, as can be seen in Fig. 1. The angular distribution measurement also indicates that the hot band transition of band *I* is overlapped with another state at the position of peak *k*.

The determined molecular parameters for both bands *X* and *I* are listed in Table II. The results show almost identical vibrational frequencies for the anion and both neutral states, and virtually identical geometry changes for the two transitions.

Since the two transitions are relatively vertical and only a few vibrational transitions are observed, an accurate determination of vibrational anharmonicities is impossible. For the same reason, the sign of the bond length change cannot be determined based on the simulation. We assume that the bond length of the anion ground state is smaller than that of the neutral ground and excited states ($r_e' - r_e'' > 0$). This assumption will be justified by molecular orbital arguments discussed in Sec. IV.

During the Franck–Condon fit, the FWHMs of the two bands were found to be different. The 15 meV FWHM for the ground state is significantly broader than the corresponding 11 meV value for the excited state. Calibration of the instrumental resolution on atomic transitions shows that the large difference cannot arise from any variation in reso-

TABLE II. The electronic states and molecular constants of palladium dimer.*

Molecule	Pd ₂ ⁻	Pd ₂	Pd ₂
Assignment	$X^2\Sigma_u^+$	$X^3\Sigma_u^+$	$^1\Sigma_u^+$
Configuration	$(4d^{19}\sigma_u)(5s\sigma_g)^2$	$(4d^{19}\sigma_u)(5s\sigma_g)^1$	$(4d^{19}\sigma_u)(5s\sigma_g)^1$
ω_e (cm ⁻¹)	206 ± 15	210 ± 10	200 ± 15
r_e^b (Å)	$(r_e' - 0.037) \pm 0.008$	r_e'	$(r_e' - 0.007) \pm 0.008$
T_0 (eV)	-1.685 ± 0.008	0	0.497 ± 0.008
D_0 (eV)	2.15 ± 0.17	1.03 ± 0.16^a	
E.A. (eV)		1.685 ± 0.008	

*The values are from this work except for the neutral dissociation energy which is from Shim and Gingerich (see Ref. 10).

^bThe absolute values of the bond lengths cannot be obtained from this work. A recent calculation suggests $r_e' \approx 2.48$ Å (see Ref. 12).

lution. Also, as both bands are nearly vertical, the rotational contours should both be narrow and similar. The broader linewidth of the ground state may arise from a second-order spin-orbit splitting, as discussed in detail in Sec. IV.

With the relationship $D_0(\text{Pd}_2^-) = D_0(\text{Pd}_2) + \text{E.A.}(\text{Pd}_2) - \text{E.A.}(\text{Pd})$, we can determine the anion dissociation energy. Using the third-law value of $D_0(\text{Pd}_2) = 1.03 \pm 0.16$ eV,¹⁰ along with $\text{E.A.}(\text{Pd}_2)$ and $\text{E.A.}(\text{Pd})$ from this work, the value of $D_0(\text{Pd}_2^-) = 2.15 \pm 0.17$ eV is derived. The dissociation energy of the anion dimer is twice that of the neutral dimer. This experiment directly and precisely measures the dissociation energy difference between the anion and neutral $D_0(\text{Pd}_2^-) - D_0(\text{Pd}_2) = 1.123 \pm 0.013$ eV, independent of the determination of the neutral dissociation energy.

IV. DISCUSSION

Although the photoelectron spectrum of Pd₂⁻ is the simplest of the nickel group,³³ it is much more complex than those of the coinage metal dimers.⁶ In the nickel group transition metals, the interactions of the *s* electrons are thought to dominate the bonding and electronic structure in the dimers, but the open *d* shell creates the possibility for *d* electrons to participate in bonding. Palladium dimer possesses some special properties because of its unique atomic configuration $4d^{10}5s^0$. To first order, two ground state (¹S₀) atoms interact only through a van der Waals attraction.³⁵ In order to make an *s* valence electron available for stronger σ bonding, one or both atoms must be promoted to a low-lying excited state. The interaction of a first excited state atom ³D($4d^9 5s^1$) with a ground state atom can form a stable molecule $4d^{19}(5s\sigma_g)^1$ with a bond order of 1/2. (Here we use a simplified molecular state notation, in which all the *d* electrons from the two constituent atoms are summed together and only the σ molecular orbitals are given along with the *s* electronic configurations.) However, the price paid for this bonding is a promotion energy of 6564 cm⁻¹, which could cancel a considerable part of the bond energy. Likewise, combining two ³D atoms forms a $4d^{18}(5s\sigma_g)^2$ molecule

with a bond order of 1, but the required promotion energy is consequently doubled. The mixed ³D, ¹D, and ¹S combinations can form a large number of low-lying electronic states. Thus, the determination of the Pd₂ ground state is nontrivial, as is shown by the quantum chemical calculations.^{9-12,19} The most likely ground state configurations, along with their lowest dissociation asymptotes, are listed in Table III.

Pd⁻ also has an unusual ground state ²S_{1/2}($4d^{10}5s^1$)²⁸ as well as an excited state ²D_{5/2}($4d^9 5s^2$) lying only 1113 cm⁻¹ above the ground state. In comparison, Ni⁻ and Pt⁻ possess the $nd^9(n+1)s^2$ ground state configurations.²⁶ The interaction of the ground state anion (²S_{1/2}) and the neutral atom (¹S₀) forms a molecular anion $4d^{20}(5s\sigma_g)^1$ with a bond order of 1/2. The interaction of the ground state neutral atom with the excited state anionic atom can form a $4d^{19}(5s\sigma_g)^2$ molecular anion with a σ bond order of 1; in this case, one pays a considerably smaller promotion energy than for the neutral. The interaction of the ground state atomic anion with the excited state neutral atom can also form a bonding molecule, but pays the same 6564 cm⁻¹ promotion energy as in the neutral case. Finally, combining the lowest excited states of the atomic anion and the Pd atom forms a $4d^{18}(5s\sigma_g)^2(5s\sigma_u)^1$ molecule with a bond order of 1/2. All the likely anion ground states are listed in Table III. At this level of analysis, the ground state configuration is not obvious.

The photoelectron spectrum provides rich information about the electronic and vibrational structure and the molecular orbitals. Relying on this information, we can attempt to assign the ground state of both the anion and neutral dimers. When assigning the possible transitions, it is important to note two major propensity rules of electron photodetachment:^{28,36} (1) generally, single electron processes (i.e., detachment with no additional electron reorganization) are expected to give rise to the strongest photoelectron transitions; (2) processes involving *s* electron detachment are expected to have larger cross sections (within 1–2 eV above threshold) than those involving *d* electron detachment.

TABLE III. Configurations of low-lying molecular states of Pd₂⁻ and Pd₂, with their dissociation asymptotes and corresponding atomic promotion energies.

Configuration	Asymptote	Promotion energy ^a (cm ⁻¹)	Bond order	Spin
Pd₂				
$d^{20}s^0$	¹ S ₀ (d^{10}) + ¹ S ₀ (d^{10})	0	0	<i>S</i> = 0
$d^{19}(s\sigma_g)^1$	¹ S ₀ (d^{10}) + ³ D ₃ ($d^9 s$) ^b	6 564	1/2	<i>S</i> = 1
	¹ S ₀ (d^{10}) + ¹ D ₂ ($d^9 s$)	11 721	1/2	<i>S</i> = 0
$d^{18}(s\sigma_g)^2$	³ D ₃ ($d^9 s$) + ³ D ₃ ($d^9 s$)	13 128	1	<i>S</i> = 0,1
Pd₂⁻				
$d^{20}(s\sigma_g)^1$	¹ S ₀ (d^{10}) + ² S _{1/2} ($d^{10} s$)	0	1/2	<i>S</i> = 1/2
$d^{19}(s\sigma_g)^2$	¹ S ₀ (d^{10}) + ² D _{5/2} ($d^9 s^2$) ^b	1 113	1	<i>S</i> = 1/2
	³ D ₃ ($d^9 s$) + ² S _{1/2} ($d^{10} s$)	6 564	1	<i>S</i> = 1/2,3/2
$d^{18}(s\sigma_g)^2(s\sigma_u)^1$	³ D ₃ ($d^9 s$) + ² D _{5/2} ($d^9 s^2$)	7 677	1/2	<i>S</i> = 1/2,3/2

^aThe values are from Ref. 18 except for the energy level of the Pd⁻ first excited state which is from this work.

^bThe ground state assigned in this work.

Based on these rules, we attribute the strongest transitions *X* and *I* to *s*-like detachments. This assignment is consistent with the angular distribution measurements discussed earlier.

For the anion, the state with the $4d^{18}(5s\sigma_g)^2(5s\sigma_u)^1$ configuration (in Table III) is the least likely for the ground state in terms of the high promotion energy and the low σ bond order as mentioned above. Additionally, if $4d^{18}(5s\sigma_g)^2(5s\sigma_u)^1$ were the ground state, the anion bond energy would not be larger than that of the neutral, as one $s\sigma_u$ electron would be expected to be detached in the photoelectron process. Such an assignment would be in disagreement with the experimental finding that $D_0(\text{Pd}_2^-) > D_0(\text{Pd}_2)$ and thus can be excluded. Another unfavorable candidate is $4d^{20}(5s\sigma_g)^1$. This configuration goes to the neutral $4d^{20}5s^0$ by detaching an $s\sigma_g$ electron. The measured vibrational frequency of the neutral ground state (210 cm^{-1}) is definitely too high for this weakly bound state.¹² The remaining possibility is the $4d^{19}(5s\sigma_g)^2$ configuration, which has two possible dissociation asymptotes, as indicated in Table III. The first one, which is correlated to the lower energy asymptote, is most likely considering the low promotion energy. Only 1113 cm^{-1} promotion energy is paid for this bonding state, but the reward is a full σ bond. The process of $s\sigma_g$ electron detachment is consistent with the experimental dissociation energies, transition intensities, and angular distribution measurements. Based on these arguments, the state with the $4d^{19}(5s\sigma_g)^2$ configuration and correlated to the $^1S_0(d^{10}) + ^2D_{5/2}(d^9s^2)$ dissociation asymptote is assigned to the ground state of Pd₂⁻. It should be noted that the ground state dissociation energy D_0 refers to the lowest (adiabatic) dissociation asymptote $^1S_0(d^{10}) + ^3D_3(d^{10}s^1)$. The direction of the bond length changes in the *X* and *I* bands can now be determined based on the anion ground state assignment. The bond strength is expected to decrease with $s\sigma_g$ electron detachment, causing the bond length to increase. On this basis, we used a larger neutral bond length ($r'_e - r''_e > 0$) for the Franck-Condon analysis.

The analysis described in Sec. III indicates that the *X* and *I* states are almost identical in terms of their transition intensities, bond length changes, vibrational frequencies, and photoelectron angular distributions. This strongly suggests that two transitions arise from the same $5s\sigma_g$ electron detachment. Having determined the anion ground state, we find that the only possible transition to the neutral ground state is $4d^{19}(5s\sigma)^1 + e^- \leftarrow 4d^{19}(5s\sigma)^2$. The $4d^{18}(5s\sigma)^2 + e^- \leftarrow 4d^{19}(5s\sigma)^2$ transition cannot be the ground to ground state transition because it corresponds to *d* electron detachment, a process inconsistent with both the angular distribution and intensity of band *X*. The configurations and dissociation asymptotes in Table III show that $5s\sigma_g$ detachment transitions lead to singlet and triplet final states, depending on the spin-spin coupling between the one *s* valence electron and the *d* electrons. If we assume that the *4d* orbitals are bonding and in ordinary order, then we expect that one *d* electron is excited from $4d\sigma_u$ to $5s\sigma_g$, corresponding to atomic $^1S \rightarrow ^3D$, 1D promotions. The neutral MO valence configuration can be written as

$4d^{19}5s^1(1\sigma_g^2\delta_g^4\delta_u^4\pi_u^4\pi_g^41\sigma_u2\sigma_g)$ or $(1\sigma_u2\sigma_g)$ for short. Using $\Lambda-\Sigma$ (case a) coupling, we obtain the triplet state $^3\Sigma_u^+$ and the singlet state $^1\Sigma_u^+$. Since the parallel-spin triplet state is usually more stable than the antiparallel-spin singlet state, we believe $^3\Sigma_u^+$ to be the ground state. Applying this assignment to the photoelectron spectrum, we assign bands *X* and *I* to the $^3\Sigma_u^+$ and $^1\Sigma_u^+$ states, respectively. If we consider the spin-orbit effect, $\Omega-\Omega$ (case c) coupling must be employed, which results in the $^3\Sigma_u^+$ ground state splitting into 0_u^- and 1_u^- . Using the same method, we determine the ground state of Pd₂⁻ to be $^2\Sigma_u^+$ in terms of $\Lambda-\Sigma$ coupling with the molecular orbital configuration $4d^{19}5s^2(1\sigma_g^2\delta_g^4\delta_u^4\pi_u^4\pi_g^41\sigma_u2\sigma_g^2)$ or $(1\sigma_u2\sigma_g^2)$.

Balasubramanian recently calculated¹² the energies of the Pd₂ low-lying electronic states. He found 41 low-lying electronic states within 9000 cm^{-1} of the ground state; this energy range corresponds to the spectral region between bands *X* and *III*. Although this calculation does not include all possible low-lying electronic states, the state density is still higher than that observed in the photoelectron spectrum, particularly in the region between band *X* and *I*. The reason we observe fewer electronic states in the spectrum is because of photodetachment selection rules.

The *ab initio* calculations predict¹² the ground state to be $^3\Sigma_u^+(1\sigma_u2\sigma_g)$ and that the $^3\Sigma_u^+$ state is split by 9 cm^{-1} into 1_u and 0_u^- states, with 1_u as the ground state. The energy splitting between $^3\Sigma_u^+(1_u)$ and $^1\Sigma_u^+(0_u^+)$ is predicted to be 4443 cm^{-1} . Our assignment of bands *X* and *I* yields a triplet-singlet splitting of $0.497 \pm 0.008\text{ eV}$ ($4008 \pm 65\text{ cm}^{-1}$), which is in agreement with Balasubramanian's calculations. The spin-orbit splitting of 9 cm^{-1} is too small to be resolved in our spectrum, but may broaden the linewidth of band *X*. We found the linewidth of band *X* to be 4 meV (32 cm^{-1}) broader than that of *I*, which suggests that the observed broadening of band *X* could be attributed to the spin-orbit splitting. Our measurement confirms qualitatively the *ab initio* calculation, but suggests that the theoretical calculation of 9 cm^{-1} may be an underestimate and that the actual spin-orbit splitting of the $^3\Sigma_u^+$ state could be as large as 30 cm^{-1} . Assuming that the transition intensities for the two states $^3\Sigma_u^+(1_u)$ and $^3\Sigma_u^+(0_u^-)$ are nearly the same, we then see that the transition origin for the ground state (1_u) may be $1\text{--}2\text{ meV}$ lower than the value obtained from the Franck-Condon analysis. With this spin-orbit correction, we determine the new adiabatic electron affinity of E.A.(Pd₂) to be $1.685 \pm 0.008\text{ eV}$.

The vibrational frequencies of the anion and neutral ground states appear to be nearly the same, while the dissociation energy for the anion is much larger than for the neutral. The vibrational frequency of Pd₂⁻ (206 cm^{-1}) is comparable to that of isoelectronic Ag₂ (192 cm^{-1}).¹ Both Pd₂⁻ and Ag₂ possess a full σ bond and have nearly the same mass, so the magnitude of their frequencies may reflect the σ bond strength. The vibrational frequencies of *X* ($^3\Sigma_u^+$) and $^1\Sigma_u^+$ from Balasubramanian's calculations¹² are $\approx 25\%$ smaller than those reported here. Lee *et al.*¹⁹ predicted ω_e to be 222 cm^{-1} for the ground state *X* ($^3\Sigma_u^+$); this theoretical value is in close agreement with our result.

Detailed spectral analysis of the other peaks and bands is difficult because of spectral congestion and the lack of established electronic and vibrational information. Only a qualitative explanation is attempted here. The intensities of peaks *f*, *g*, and *h* are weaker than those of bands *X* and *I*. Asymmetry parameters of ≈ 1.5 are obtained for all three peaks, indicating that these peaks result from $s\sigma_g$ electron detachment. However, the only possible single electron transitions resulting from $s\sigma_g$ electron detachment have been assigned to bands *X* and *I*. Therefore we must invoke a two-electron mechanism. Earlier, we stated that single electron processes should dominate the photodetachment transition. This propensity is likely to become less valid for heavy transition metal dimer anions, due to the enhanced effects of electron correlation in these systems. Pd₂⁻ is a multi-*d*-electron system and the electron correlation is expected to be important. *Ab initio* calculations show that most of the low-lying electronic states of Pd₂ are quite mixed in character, owing to strong configuration interaction.¹² This effect may result in transitions arising from two-electron processes: one $s\sigma_g$ electron detachment accompanied by reorganization of the *d* electrons. A similar two-electron process was observed in the Pd⁻ photoelectron spectrum.²⁸ There are many possible low-lying neutral excited states which may correspond to peaks *f*, *g*, and *h*. These states must have the same electronic configuration as the ground state, but different *d*-electron arrangements, such as $4d^{19}5s^1(2\sigma_g\delta_u^3$ or $2\sigma_g\pi_g^3)$. Balasubramanian¹² calculated the energies of some states, such as $^3\Delta_u$ and $^1\Delta_u$ with a $2\sigma_g\delta_u^3$ configuration and $^3\Pi_g$ and $^1\Pi_g$ with a $2\sigma_g\pi_g^3$ configuration. Relying on his calculation, we would say that $^3\Pi_g$ is the lowest excited electronic state (Λ - Σ coupling) observed in the photodetachment experiment, and that peaks *f*, *g*, and *h* can be tentatively assigned to the spin-orbit states $^3\Pi_g(1_g)$, $^3\Pi_g(0_g^-)$, and $^3\Pi_g(0_g^+)$, respectively.

The weak intensities and negative β of the remaining peaks or bands (*i*, *j*, *k*, *II*, and *III*) suggest that these peaks arise from *d*-electron detachment. Detaching a *d* electron from the anion can be written as $4d^{18}(5s\sigma)^2 \leftarrow 4d^{19}(5s\sigma)^2$. These photoelectron transitions could be more numerous than *s* photodetachment transitions, since *d* electrons can be detached from three different molecular orbitals, i.e., $d\sigma_u$, $d\pi_g$, and $d\delta_u$. Furthermore, two-electron processes (one *d*-electron detachment with another *d* electron reorganization) could possibly give rise to additional photoelectron transitions. Balasubramanian calculated the energies for the neutral excited states $4d^{18}(5s\sigma)^2$ with numerous MO configurations, e.g., $1\sigma_u\delta_u^3$ or $1\sigma_u\pi_g^3$. Many states lie between the $^3\Sigma_u^+$ and $^1\Sigma_u^+$ states or just above the $^1\Sigma_u^+$ state, where *i*, *j*, *k*, *II*, and *III* are observed in our spectrum. However, the spectral complexity makes a detailed assignment infeasible at the present time.

In addition to the bands and peaks discussed above, poorly resolved features in the region of 2.6–3.3 eV, or ≈ 8000 cm⁻¹ above the ground state, appear in the spectrum. These features can be attributed to a large number of weak transitions, because a high density of electronic states is predicted⁷ 10 000 cm⁻¹ above the ground state. The Morse group has attempted two-photon ionization spectroscopy

copy of gas phase Pd₂.¹⁷ They scanned the spectral region from 11 375 to 23 000 cm⁻¹ and no transitions were observed. They concluded that Pd₂ photoabsorption certainly occurs in their scanning range, but efficient predissociation prevented Pd₂⁺ detection with the resonant two-photon ionization technique. The features in the photoelectron spectrum are not inconsistent with the predissociation mechanism. Generally, when photodetachment occurs, photoelectron signals should be detected regardless of the following predissociation; however, many repulsive states lie 1 eV above the ground state and slice through all the bound states lying in the same region: in the photodetachment process, the molecules excited to these bound states could undergo fast predissociation. This process is so fast that the corresponding transition could be equivalent to a bound-free transition. The transition intensity is proportional to the Franck–Condon factors and the Franck–Condon factors for a bound-free transition are much smaller than for a bound-bound transition. Therefore we observe the high density of electronic transitions 1 eV above the ground state and all of these transitions are weaker than those of the labeled peaks and bands in the low energy region.

A comparison of the palladium dimer with the nickel, platinum, and copper group metal dimers^{6,7} indicates that there are dramatic differences between the palladium dimer and the other dimers. For nickel, platinum, and the coinage metal dimers, the electronic configurations of the anion and the neutral are $nd^m[(n+1)(s\sigma_g)^2(s\sigma_u)]$ and $nd^m[(n+1)(s\sigma_g)^2]$ (where $m = 18$ for Ni and Pt, $m = 20$ for the coinage metals). The bond strengths of the neutral dimers are larger than those of the anion dimers,^{6,33} as predicted from the MO configurations. The MO configurations of the palladium anion and neutral dimers assigned in this work are $4d^{19}(5s\sigma_g)^2$ and $4d^{19}(5s\sigma_g)^1$, respectively. In addition, the dissociation energy of Pd₂⁻ is twice that of Pd₂. The reason for the unusually small dissociation energy of the neutral dimer compared to the other nickel group and coinage metal dimers is the extra promotion energy required for *s* σ bonding.

V. CONCLUSIONS

The negative ion photoelectron spectra of Pd⁻ and Pd₂⁻ have been obtained using 351.1 nm (3.531 eV) laser radiation at an instrumental resolution of 9–10 meV. These experiments yield precise electron affinities for E.A.(Pd) and E.A.(Pd₂) and provide direct information on the ground and low-lying electronic states of gas phase Pd₂.

The spectrum exhibits multiple low-lying electronic states of Pd₂ and the vibrational structure is resolved for two of these low-lying electronic states. The spectrum displays two strong electronic bands; they show nearly identical vibrational frequencies, Franck–Condon intensities, and photoelectron angular distributions. With the help of simple molecular orbital arguments and *ab initio* calculations, these two electronic bands are assigned to the triplet ground state ($^3\Sigma_u^+$) and a singlet excited state ($^1\Sigma_u^+$). These states have identical electronic configurations $4d^{19}(5s\sigma)^1$ and differ in

the spin coupling of the $5s\sigma_g$ electron to the d -electron hole. The adiabatic electron affinity is determined to be $E.A.(Pd_2) = 1.685 \pm 0.008$ eV and the singlet excitation energy is found to be 0.497 ± 0.008 eV. The experiment also precisely measures the increase in dissociation energy upon anion formation $D_0(Pd_2^-) - D_0(Pd_2) = 1.123 \pm 0.013$ eV.

The configurations of the neutral and anion ground states are determined, respectively, as $4d^{19}(1\sigma_g^2\delta_g^4\delta_u^4\pi_u^4\pi_g^41\sigma_u)5s^1(2\sigma_g)$ and $4d^{19}(1\sigma_g^2\delta_g^4\delta_u^4\pi_u^4\pi_g^41\sigma_u)5s^2(2\sigma_g^2)$. The anion bond strength is found to be twice that of the neutral ground state, while the vibrational frequencies and bond lengths are nearly the same. The reason for the unusually small dissociation energy of the neutral dimer is the extra promotion energy paid for $s\sigma$ bonding. Therefore, the special character of palladium dimer can be attributed to the unique stable ground state $^1S_0(4d^{10}5s^0)$ of the palladium atom.

The electronic structures of Ni₂ and Pt₂, for which studies are in progress, are expected to provide interesting contrasts.

ACKNOWLEDGMENTS

This research was supported by the National Science Foundation, Grants No. CHE88-19444 and No. PHY90-12244.

¹ M. D. Morse, *Chem. Rev.* **86**, 1049 (1986).

² M. Moskovits, *Metal Clusters* (Wiley, New York, 1986).

³ J. Koutecký and P. Fantucci, *Chem. Rev.* **86**, 539 (1986); W. Weltner, Jr. and R. J. VanZee, *Annu. Rev. Phys. Chem.* **35**, 291 (1984).

⁴ J. L. Gole and W. C. Stwalley, *Metal Bonding and Interactions in High Temperature Systems: with Emphasis on Alkali Metals* (American Chemical Society, Washington D.C., 1982), ACS Symp. Sec. 179; J. L. Gole, R. H. Childs, D. A. Dixon, and R. A. Eades, *J. Chem. Phys.* **72**, 6368 (1980).

⁵ K. M. Ervin and W. C. Lineberger, in *Advances in Gas Phase Ion Chemistry*, edited by N. G. Adams and L. M. Babcock (JAI, Greenwich, Conn., in press), Vol. 1.

⁶ J. Ho, K. M. Ervin, and W. C. Lineberger, *J. Chem. Phys.* **93**, 6987 (1990).

⁷ M. D. Morse, *Advances in Metal and Semiconductor Clusters* (in press).

⁸ T. H. Upton and W. A. Goddard III, *J. Am. Chem. Soc.* **100**, 5659 (1978); I. Shim, J. Dahl, and H. Johansen, *Int. J. Quantum Chem.* **15**, 311 (1979); J. O. Noell, M. D. Newton, P. J. Hay, R. L. Martin, and F. W. Bobrowicz, *J. Chem. Phys.* **73**, 2360 (1980).

⁹ H. Basch, D. Cohen, and S. Topoil, *Isr. J. Chem.* **19**, 233 (1980).

¹⁰ I. Shim and K. Gingerich, *J. Chem. Phys.* **80**, 5107 (1984).

¹¹ D. R. Salahub, in *Proceedings of the Nobel Laureate Symposium on Applied Quantum Chemistry*, edited by V. H. Smith, Jr., H. F. Schaeffer III, and K. Morokuma (Deidel, Dordrecht, 1986).

¹² K. Balasubramanian, *J. Chem. Phys.* **89**, 6310 (1988).

¹³ K. Balasubramanian, *J. Chem. Phys.* **87**, 6573 (1987).

¹⁴ M. D. Morse, G. P. Hansen, P. R. R. Langridge-Smith, L.-S. Zheng, M. E. Geusic, D. L. Michalopoulos, and R. E. Smalley, *J. Chem. Phys.* **80**, 5400 (1984).

¹⁵ S. Taylor, G. W. Lemire, Y. Hamrick, Z.-W. Fu, and M. D. Morse, *J. Chem. Phys.* **89**, 5517 (1988).

¹⁶ S. Taylor, E. M. Spain, and M. D. Morse, *J. Chem. Phys.* **92**, 2698 (1990).

¹⁷ S. Taylor, E. M. Spain, and M. D. Morse, *J. Chem. Phys.* **92**, 2710 (1990).

¹⁸ C. E. Moore, *Atomic Energy Levels* (Nat'l. Bur. Stand. U.S. Government Printing Office, Washington, D.C., 1952), Circ. 467.

¹⁹ S. Lee, D. M. Bylander, and L. Kleinman, *Phys. Rev. B* **39**, 4916 (1988).

²⁰ S. S. Lin, B. Strauss, and A. Kant, *J. Chem. Phys.* **51**, 2282 (1969).

²¹ D. G. Leopold, J. Ho, and W. C. Lineberger, *J. Chem. Phys.* **86**, 1715 (1987).

²² K. M. Ervin, J. Ho, and W. C. Lineberger, *J. Chem. Phys.* **89**, 4514 (1988).

²³ C. S. Feigerle, Ph.D. thesis, University of Colorado, 1983.

²⁴ D. G. Leopold, K. K. Murray, A. E. Stevens Miller, and W. C. Lineberger, *J. Chem. Phys.* **83**, 4849 (1985).

²⁵ K. M. Ervin, J. Ho, and W. C. Lineberger, *J. Chem. Phys.* **91**, 5974 (1989).

²⁶ H. Hotop and W. C. Lineberger, *J. Phys. Chem. Ref. Data* **14**, 731 (1985).

²⁷ J. Cooper and R. N. Zare, *J. Chem. Phys.* **48**, 942 (1968).

²⁸ C. S. Feigerle, R. R. Corderman, S. V. Bobashev, and W. C. Lineberger, *J. Chem. Phys.* **74**, 1580 (1981).

²⁹ K. M. Ervin and W. C. Lineberger, *J. Phys. Chem.* **95**, 1197 (1991).

³⁰ M. K. Gilles, K. M. Ervin, J. Ho, and W. C. Lineberger, *J. Chem. Phys.* (submitted).

³¹ J. L. Hall and M. W. Siegel, *J. Chem. Phys.* **48**, 943 (1968).

³² A. Kasdan and W. C. Lineberger, *Phys. Rev. A* **10**, 1658 (1974).

³³ J. Ho and W. C. Lineberger (unpublished experimental results).

³⁴ V. M. Bierbaum, G. B. Ellison, and S. R. Leone, in *Gas Phase Ion Chemistry*, edited by M. T. Bowers (Academic, New York, 1984), Vol. 3, p. 1.

³⁵ *Ab initio* calculations predict that the state $^1\Sigma_g^+(4d^{20}5s^0)$ can be a weakly bound state with a vibrational frequency of 120 cm^{-1} ; see Ref. 12.

³⁶ (a) R. R. Corderman, P. C. Engelking, and W. C. Lineberger, *J. Chem. Phys.* **70**, 4474 (1979); (b) P. C. Engelking and W. C. Lineberger, *Phys. Rev. A* **19**, 149 (1979).